ELSEVIER

Soil Dynamics and Earthquake Engineering 22 (2002) 781–790

SOIL DYNAMICS AND EARTHQUAKE ENGINEERING

www.elsevier.com/locate/soildyn

# Characteristics of strong ground motion during the 1999 Chi-Chi earthquake (Taiwan) and large aftershocks: comparison with the previously established models

Vladimir Sokolov[a,*], Chin-Hsiung Loh[b], Kuo-Liang Wen[c]

[a]Geophysical Institute, Karlsruhe University, Hertzstr. 16, 76187, Karlsruhe, Germany
[b]National Center for Research on Earthquake Engineering, 200, Sec. 3, Hsinhai Road, Taipei, Taiwan, ROC
[c]Institute of Applied Geology, National Central University, 38, Wu-chuan Li, Chung-li, Taiwan, ROC

**Abstract**

In the Taiwan region, the empirical spectral models for estimating ground motion parameters were obtained recently on the basis of recordings of small to moderate ($5.0 \le M_L \le 6.5$) earthquakes. A large collection of acceleration records from the recent $M_L$ 7.3 ($M_W$ 7.6) Chi-Chi earthquake (20 September, 1999) makes it possible to test the applicability of the established relationships in the case of larger events. The comparison of ground motion parameters (peak accelerations and response spectra), which were calculated using the stochastic approach based on the modeled Fourier amplitude spectra, and the observed data demonstrates that the models may be successfully used for ground motion prediction for earthquakes of magnitudes up to $M_L = 6.8–7.0$ and hypocentral depth more than 10 km. To satisfy to the peculiarities of ground motion during shallow (depth less than 10 km) and larger ($M_L > 7.0$) events, the models were revised.


*Keywords:* Chi-Chi earthquake; Acceleration spectra; Ground motion modeling

## 1. Introduction

Procedures of seismic hazard assessment are based on ground motion attenuation relationships, which should consider regional earthquake source and propagation path effects and local site response peculiarities. However, the empirical databases, which are used for evaluation of the relationships, usually consist of the recording which were obtained during the events of small and moderate magnitudes. Therefore, a question is arising—"is it possible to use these relationships in the case of larger events?" Every strong earthquake provides an unique opportunity to verify the accepted attenuation models and to update empirical relationships. The most expressive example of such informative events is the recent Chi-Chi (Taiwan) $M_W = 7.6$ earthquake which produced a rich set of strong ground motion recordings [1].

In recent years, Fourier-amplitude spectrum is widely used for prediction of ground motion parameters [2–5] on the basis of stochastic technique [6]. In one of the frequently used approaches, the spectrum is represented by analytical expressions describing source, propagation, and site effect, separately [6–11]. These models (very simple or complicated) revealed some common features reflecting the source mechanism and travel-path influence, however, different regional and local conditions may produce significant differences in spectral contents of the ground-motion records. In the Taiwan region, the empirical spectral models for estimating ground motion parameters were obtained recently on the basis of recordings of small to moderate ($5.0 \le M_L \le 6.5$) earthquakes [12]. A large collection of acceleration records from the recent $M_L = 7.3$ Chi-Chi earthquake and its large ($M_L > 6.5$) aftershocks (more than 1000 records obtained at distances up to 120–140 km) allows us to test the applicability of the established relationships in the case of large shallow thrust earthquakes.

In this paper, we compare the ground motion parameters (Fourier amplitude spectra, peak accelerations and response spectra) which were estimated for average soil conditions using the previously established models, and the data observed during the Chi-Chi earthquake and aftershocks.

* Corresponding author. Fax: +49-721-71173.
*E-mail address:* vladimir.sokolov@gpi.uni-karlsruhe.de (V. Sokolov).


PII: S0267-7261(02)00099-4

## 2. Empirical spectral model for the Taiwan region

The model considered in this study is represented by the empirical spectra of ground acceleration estimated for reference distance $R = 1$ km (Fig. 1(a), solid lines). These empirical spectra were obtained on the basis of acceleration records (the most significant part of the records, starting from S-wave arrival) in the Taiwan region for magnitude ranges $5.0 < M_L < 5.5$; $5.5 < M_L < 6.0$, and $6.0 < M_L < 6.5$ and, averaging the variety of site conditions from rock sites to soft soils of different thickness, correspond to the so-called 'average soil' [12]. The spectrum at a given distance $R$ ($A_R$) is calculated from the 'reference distance' spectra ($A_{R=1}$) as

$$A_R(f) = A_{R=1}(f)R^b \exp[-\pi f R/Q(f)\beta] \quad (1)$$

where $b = -1.0$ for distances $R < 50$ km and $b = 0.0$ for $50 < R < 150–170$ km; $\beta$ is the shear wave velocity in the earth's crust (3.6 km/s); $Q(f) = 225f^{1.1}$ for deep (depth more than 35 km) earthquakes and $Q(f) = 125f^{0.8}$ for shallow earthquakes. In order to extend the model for the larger magnitudes, the logarithmic increments ($\gamma_M$) of spectral amplitudes per unit of magnitude were calculated for frequencies 0.2–12 Hz in the following form

$$\gamma_M(f) = \Delta \log A(f)/\Delta M \quad (2)$$

where $\Delta M$ is the increment of magnitude between the above mentioned magnitude ranges, and $A(f)$ the reference distance spectral amplitudes (mean values, Fig. 1(a)). Fig. 1(b) shows the values $\gamma_M$ which were determined using the empirical average soil spectra for the Taiwan region and the averaged values which were used for estimation of spectral amplitudes for the larger magnitudes ($6.5 < M_L < 7.0$ and $7.0 < M_L < 7.5$, Fig. 1(a), dashed lines). The distribution of $\gamma_M$ values versus frequency shows that the values of $\gamma_M$ increase with decreasing of the frequency and they are nearly constant in low-frequency range. In other words, as the source energy increases, the intensity of low-frequency vibrations increases more rapidly than that of high-frequency vibrations. The fact agrees with the results of the previous studies of the $\gamma_M$ coefficients [13,14] on the basis of empirical data obtained in various seismic regions (California, northern Italy, Caucasus, and Central Asia).

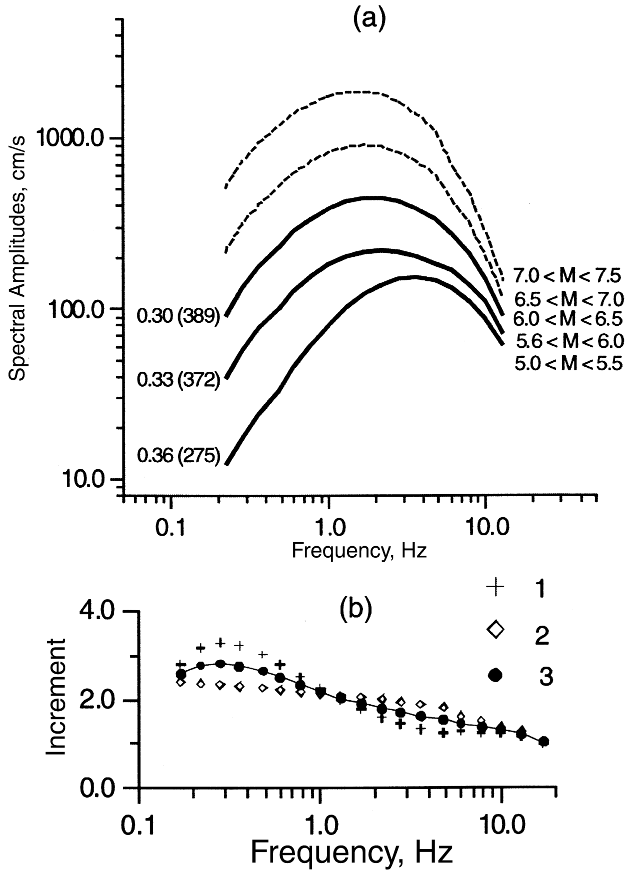


Fig. 1. Average soil spectral model (Taiwan region) for various intervals of magnitude $M$. (a) Empirical spectra (solid lines) calculated for reference distance $R = 1$ km. Numbers near the curves denote standard deviation and number of the used records (in parenthesis). Dashed lines show the spectra, which were estimated using the coefficients $\gamma_M$ (see text). (b) Frequency dependence of the coefficients $\gamma_M$ (logarithmic increment of spectral amplitudes) calculated using different intervals of magnitude ((1) $5.5 < M < 6.0$ versus $5.0 < M < 5.5$; (2) $6.0 < M < 6.5$ versus $5.5 < M < 6.0$; (3) averaged values).

## 3. The Chi-Chi earthquake data

In our study we used the data from three events (the mainshock and two largest aftershocks, Table 1). Fig. 2 shows epicenters of the earthquakes and locations of free-field, three-component, accelerograph stations recordings of which are considered. It is necessary to note that the most part of the stations to the west and south from the epicenter (CHY, KAU and TCU arrays) are located in deep alluvium plain area (the Western Coastal (WCP)). The long-period waveforms that include significant surface waves appear to be the common ground motion characteristics in the area [15,16].

Faulting during the earthquake was interpreted as reverse, left-lateral faulting on a low-angle north–south trending plane. One of the models that was used in this study (Yagi and Kikuchi, Earthquake Research Institute, University of Tokyo, Japan; see http://wwweic.eri.u-tokyo.ac.jp/yuji/taiwan/taiwan.html) is as follows: strike 3°; dipping angle 29° to the east; length of the source 90 km and width 45 km. The surface faulting produced by the earthquake (Chelungpu fault, Fig. 2) extends north–south about 96 km, and has a maximum horizontal slip of about 10 m and a maximum scarp height about 8 m. When calculating the modeled spectra by Eq. (1), we used the shortest distance between the source plane (surface of fault slippage) and the station. The sources of the aftershocks were also modeled as the planes (length 50 km; width 30 km) with the similar, as in the case of the mainshock, dipping and strike angles.

Table 1
Parameters of the Chi-Chi earthquake mainshock and aftershocks, recordings of which are used in this study

| Earthquake code | Date and time (UT) | Latitude, N | Longitude, E | Depth (km) | $M_L$ ($M_W$) | Number of records |
|---|---|---|---|---|---|---|
| Mainshock | 1999/09/20, 17:47:15 | 23°51.15′ | 120°48.93′ | 6.0 | 7.3 (7.7) | 314 |
| EQ92106 | 1999/09/22, 00:14:40 | 23°49.58′ | 121°02.80′ | 15.6 | 6.8 (6.4) | 360 |
| EQ92107 | 1999/09/25, 23:52:49 | 23°51.56′ | 121°00.35′ | 9.9 | 6.8 (6.4) | 350 |

The centers of the source planes coincide with the reported hypocenters.

## 4. Comparison of empirical and modeled data

### *4.1. Fourier amplitude spectra, the Chi-Chi earthquake aftershocks*

Magnitudes of the considered aftershocks (Table 1) lay within the first interval of magnitudes ($6.5 < M_L < 7.0$), for which the average soil spectra were evaluated using the coefficients $\gamma_M$. The Fourier amplitude spectra of ground acceleration registered during the events were initially divided into groups only by means of distance (25–35, 45–55 km, etc.) and the modeled spectra were calculated for centers of the intervals. In the case of aftershock EQ92106 ($M_L = 6.8$, hypocentral depth 15 km), the attenuation relation $Q = 125f^{0.8}$ was used. The comparison between the modeled and observed spectra for the aftershock shows a good agreement (Fig. 3(a)). Preliminary analysis of the data from aftershock EQ10297 ($M_L = 6.8$, hypocentral depth 10 km) showed that the high-frequency amplitudes of the observed spectra are characterized by more rapid decrease with distance than those predicted by the model with attenuation $Q = 125f^{0.8}$ (Fig. 3(b)). Therefore, we estimated a new $Q$-model using the approach applied in our previous study [12], and it has been found that the use of attenuation $Q = 80f^{0.8}$, reveal a better agreement between modeled and observed spectra (Fig. 3(b)). However, when the sets of empirical spectra include the recording from deep alluvium plain area (WCP, arrays CHY, KAU and TCU), the modeled spectra exhibit the smaller amplitudes than the empirical ones at frequencies less than 1–2 Hz.

Fig. 3(c) shows a typical relation between the spectra observed in the eastern part (arrays HWA, ILA and TTN) and the western part of the island (arrays CHY, TCU and KAU). The stations located in deep alluvium plain area (the WCP) are characterized by the higher spectral amplitudes at frequencies less than 1 Hz than those for eastern direction. It is naturally to suppose that the difference reflects the influence of deep deposits on ground motion. For aftershock EQ92106, the ratio between the western and eastern spectra (Fig. 3(d)) increases with the decrease of frequency (up to 2.8–2.5 at frequencies about 0.1–0.2). However, for shallow aftershock EQ92107 (depth 10 km) the ratio exhibits the sufficiently higher amplitudes than that for the deeper event (aftershock EQ92106, depth 15 km) for frequencies 0.3–0.8 Hz. It is possible to suppose that the narrow-band amplification reflects the influence of relatively long-period waves during shallow earthquakes of magnitudes 6.5–7.0, or so-called ‘shallow-earthquake effect’.

### *4.2. Fourier amplitude spectra, the Chi-Chi earthquake mainshock*

Before comparison of the data from the mainshock and modeled spectra, we should make the following notes. First, when using records obtained in epicentral zone (distances less than 10–15 km), we did not include the records obtained at stations located along the Chelungpu fault because, most probably, the records reflect anomalous movement of sediments due to impact from deep faulting. We also did not include into analyses the following data: (a) several records of TCU array obtained in liquefied area [17]; (b) records obtained in the central part of the alluvium-filled Langyang basin (ILA array), which include significant

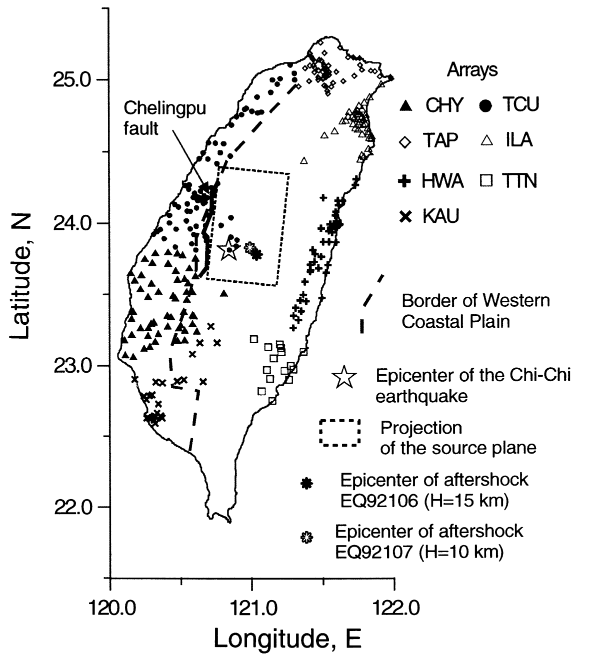


Fig. 2. Epicenters of earthquakes (the mainshock and two aftershocks), recordings of which were used in this study, and location of the free-field digital accelerograph stations (TSMIP network).

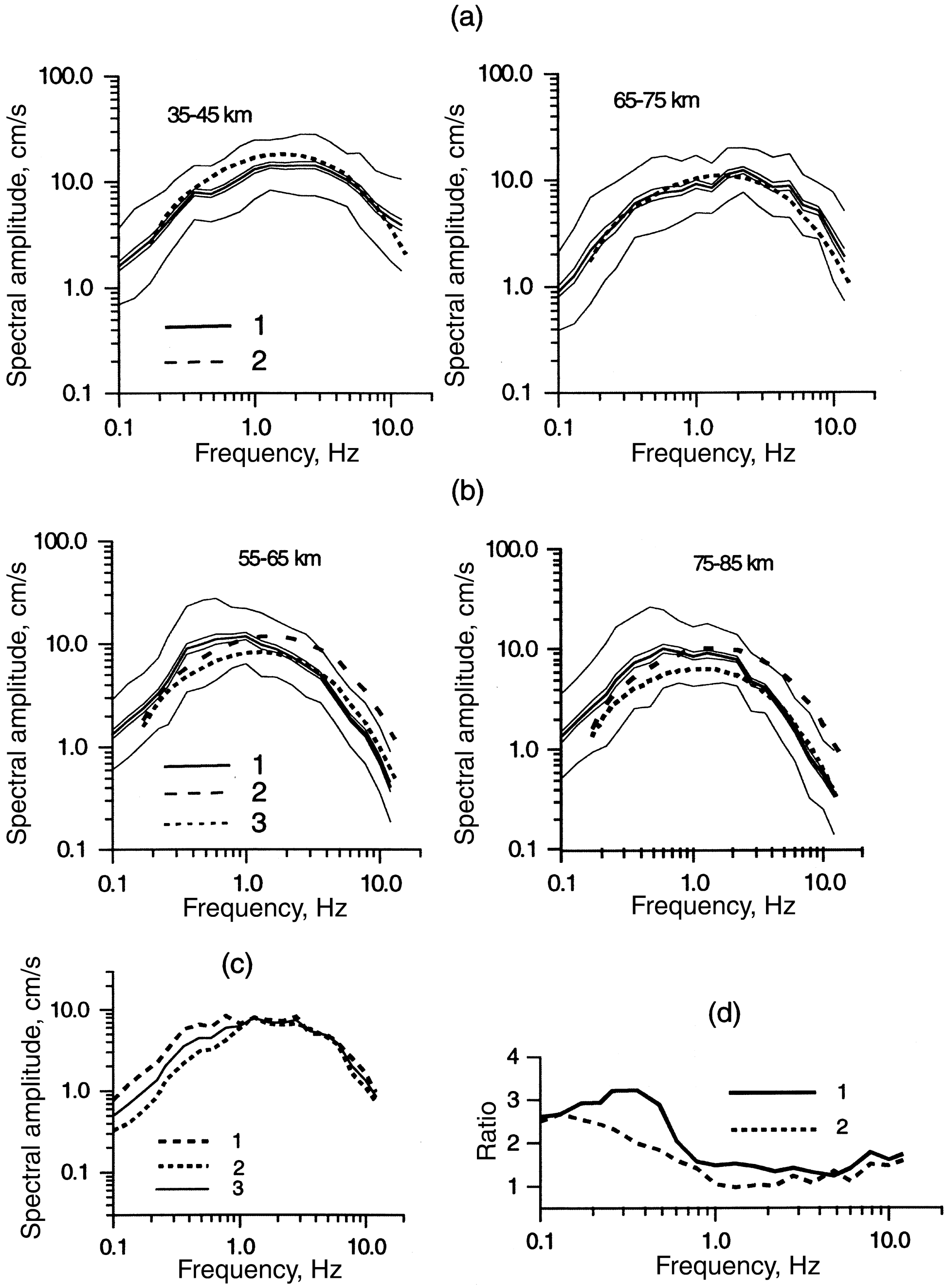


Fig. 3. The Chi-Chi earthquake aftershocks. (a) Aftershock EQ92106; 1—observed spectra (thick line—average values; thin lines—mean ± 1 st. error of means and ± 1 st. deviation limits); 2—modeled spectra (dashed lines), $Q(f) = 125f^{0.8}$ (b) aftershock EQ92107; 1—observed spectra; 2—modeled spectra, $Q(f) = 125f^{0.8}$; 3—modeled spectra, $Q(f) = 80f^{0.8}$; (c) comparison of observed spectra (EQ92106, averaged data for distance interval 75–85 km). (1) Data from WCP; (2) data from the eastern part of Taiwan island; (3) all data. (d) Ratios between observed spectra from western and eastern parts of the Taiwan island. (1) Event EQ92107; (2) event EQ92106.

surface waves; (c) records obtained in the central part of the Taipei basin (TAP array) that show a strong basin response on the earthquake. Second, we consider the accelerograms recorded in the WCP (Fig. 2) as a separate dataset due to the presence of surface waves. Third, the models of rupture process show unilateral northward propagation [15]. Therefore, we divided the data both by means of distance and direction from the source. In this case we use distance increment of 10 km and the intervals containing less than five records were not considered. The average soil spectral model (mean values) for magnitude interval $7.0 < M_L < 7.5$ was used and the modeled spectra were calculated for centers of corresponding distance intervals using two attenuation models: $Q(f) = 125f^{0.8}$ and $Q(f) = 80f^{0.8}$.

Fig. 4(a) shows the examples of comparison between simulated and observed Fourier amplitude spectra of ground acceleration. The modeled spectra calculated for correspondent distances and $Q(f) = 80f^{0.8}$ fit the mean amplitudes of observed spectra at frequencies 0.2–12 Hz both for epicentral area, eastern (HWA array) and southern direction (stations located outside WCP area). The spectra from western direction (stations of CHY and TCU arrays located in WCP), showing a good agreement with modeled spectra at frequencies more than 0.7–0.8 Hz, exhibit sufficiently larger amplitudes at frequencies less than 0.6–0.7 Hz. Obviously, the difference is caused by surface waves generated by the mainshock in this area [15,16]. At the same time, the influence of surface waves on ground motion spectra (frequencies less than 0.2–0.3 Hz) can be seen also for stations located outside the WCP at distances more than 40–50 km to the south and north from the mainshock source.

In general, the northern spectra are characterized by the highest amplitudes than the modeled spectra (and also the western and southern ones) for frequencies less than 1–2 Hz. On the one hand, this phenomenon, may be explained by the directivity effect—northward propagation of the rupture. On the other hand, the influence of propagation path peculiarities may be also considered as a source of the discrepancy. Furumura et al. [15] on the basis of numerical 2D and 3D simulation concluded that strong diving S-waves, produced by the large shallow asperity of the Chi-Chi earthquake and the large velocity gradient in the crust rigid bedrock, enhance the ground

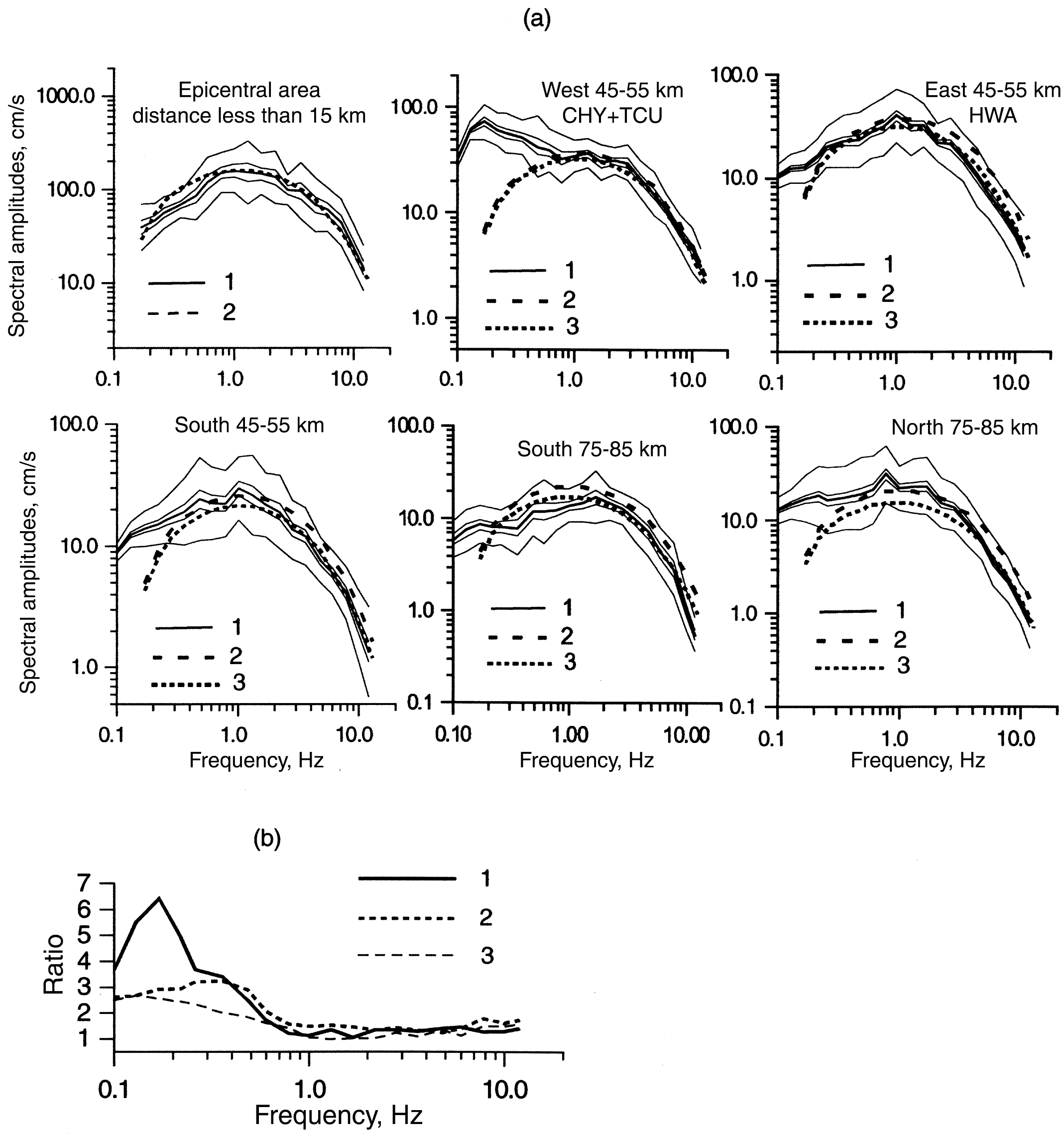


Fig. 4. The Chi-Chi earthquake mainshock. (a) Comparison of observed spectra (1, thick line—average values; thin lines—mean ± 1 st. error of means and ± 1 st. deviation limits) and modeled spectra (dashed lines, 2—$Q(f) = 125f^{0.8}$, 3—$Q(f) = 80f^{0.8}$). (b) Comparison of ratios (averaged for distances less than 50 km) between observed spectra from western and eastern part of the island. (1) The Chi-Chi earthquake mainshock; (2) aftershock EQ92107; (3) aftershock EQ92106.

motion to the north from the source at the epicentral distances around 80 and 120 km at frequency range less than 1 Hz.

Finally, let us compare the ratios of spectral amplitudes between the data from western and eastern parts of the island (west–east spectral ratios) evaluated for the considered events (mainshock and two aftershocks, for distances less than 50–55 km (Fig. 4(b)). In this case, the mainshock data do not include the above mentioned effects of rupture propagation and shallow crust structure. Therefore, the data reflect peculiarities of response of deep alluvium deposits (the WCP) during relatively large earthquakes of various depths. On the one hand, the increase of amplitudes of the ratios with decrease of frequency reflects the general characteristics of response of deep deposits on earthquake ground motion. On the other hand, the shallow (depth less than 10 km) earthquakes (mainshock and aftershock EQ92107) exhibit an additional amplification in a relatively narrow frequency band (shallow-earthquake effect). The west–east spectral ratio for the mainshock, showing approximately the same values as that in the case of aftershock EQ92107 for frequencies more than 0.4 Hz, exhibit very high amplitudes for frequencies less than 0.3 Hz. Most probably, the mainshock produced the more intensive surface waves in the WCP than aftershock EQ92107.

### *4.3. Peak ground acceleration and response spectra*

We performed the comparison of peak ground accelerations (PGA) observed during the considered events of the Chi-Chi earthquake sequence and modeled PGAs on the basis of average soil spectral models. The modeled PGA values were calculated using stochastic simulation technique [18]. One of the most important parameters of the stochastic predictions is the duration model, because it is assumed that most (90%) of the spectral energy is spread over a duration $\tau_{0.9}$ (so-called 'significant duration') of the accelerogram. It has been found in our previous study [12] that the regional relationship between ground motion duration ($\tau_{0.9}$) and magnitude proposed by Wen and Yeh [19] in the following form

$$\tau_{0.9} = 0.43\exp(0.504M_{\rm L}) \pm 2.749 \quad (3)$$

gives a better fit to empirical data. A mean value of 17 s should be used for earthquake of magnitude $M_{\rm L}$ 7.3 according to the relationship. We attempted to evaluate ground motion duration on the basis the registered accelerograms. The duration is defined as the interval between the times at which 5 and 95% of the Arias intensity integral is attained [20]. We use the average soil spectral model in our comparison; therefore it is necessary to estimate the durations excluding such extreme effects as a propagation of long-period surface waves along the alluvial basins. Thus, the high-pass filtering procedure has been applied to every accelerogram, and we calculated the duration of ground motion in the frequency range above 0.4 Hz. It has been found that, in general, duration for the mainshock reveals no dependence on the distance, at least for the northern and east–west directions from the source plane. On the other hand, the duration values for southern ground motions increase with distance and the dependence may be described as $\tau_{0.9} = 5.2R^{0.44}$. Table 2 lists the statistical parameters of ground motion duration (average value and standard deviation) determined for the entire data set, and for the stations located toward different directions from the source plane. The influence of rupture directivity could be clearly seen: the effective duration of ground motion acceleration toward the South from the source is, in general, 1.4–1.5 times higher than that toward the north. At the same time, the duration along the east–west direction may be considered as 'average' one, and the mean value of 22 s is close to that predicted by the Wen and Yeh's relationship (17 ± 2.75 s).

Fig. 5 shows the comparison between peak acceleration values observed during the mainshock (horizontal components) and those calculated using the empirical average soil spectra. A set of 40 synthetic acceleration time functions was generated for effective duration of 22 s, and the resulting PGA is estimated as an average value. In this case we consider a hypothetical situation: we have got information about the future earthquake (magnitude and source parameters) and, based on existing empirical models (average soil spectra and effective duration), the distribution of PGA values is evaluated for a scenario earthquake. The average soil model combining with effective duration that equals to 22 s, in general, provides a satisfactory prediction for the case of the Chi-Chi earthquake. However, the observed peak amplitudes at distances from 6–7 to 15–20 km are lower than the modeled values. The dataset for this distance range contains records from stations, which are located to the west from the Chelungpu fault (foot wall) and, as a rule, the footwall stations are characterized by relatively low peak acceleration as compared with that of hanging-wall location. The handing-wall near-field data marked as black squares in Fig. 5 show a good agreement with the modeled PGA. On the other hand, the modeled amplitudes are lower than the empirical ones for distances more than 60–70 km. However, the discrepancy may be explained by the above mentioned general tendency of the northern ground motion to exhibit relatively higher spectral amplitudes due to source rupture and propagation path peculiarities. When removing the northern data from analysis, the average residuals are almost equal to zero (no bias) for distances more than 20 km. The overall average value of residuals is about 0.033 for the entire data, and about −0.04 for the case when the northern data were not included. The standard deviation of residuals is about 0.20–0.22 log unit. We also modeled the peak accelerations using the mean average soil spectra plus one and two standard deviation values (Fig. 5, dashed lines). The standard deviation of average soil model for

Table 2
Results of the effective duration determination for the Chi-Chi earthquake mainshock

| Statistical parameters of the effective duration | The whole data set | Northern direction | Southern direction | E–W direction |
|---|---|---|---|---|
| Average value (s) | 22.2 | 18.2 | 30.1 | 22.0 |
| Standard deviation of $\log_{10} \tau_{0.9}$ | 0.16 | 0.09 | 0.17 | 0.15 |

magnitudes $7.0 < M_L < 7.5$ has been accepted as average (0.33 log unit) between the values for the empirical reference spectra (see Fig. 1(a)). It is seen that the mean + 1 standard deviation spectral model provides an upper limit of peak acceleration for the near field area (distances less than 30–40 km), and the mean + 2 standard deviation model also overlaps the effect of the Taipei basin response (northern data, distances 90–110 km).

The distribution of significant duration versus distance for aftershock EQ92106 reveals an increase of the duration with increasing the distance. The dependence may be described as $\tau_{0.9} = 1.29R^{0.56}$ or $\log_{10} \tau_{0.9} = (0.11 \pm 0.054) + (0.56 \pm 0.028)\log_{10} R$. Therefore, when applying the average soil spectral model (magnitude range $6.5 < M_L < 7.0$, $Q(f) = 125f^{0.8}$), the peak acceleration values were determined using the distance-dependent

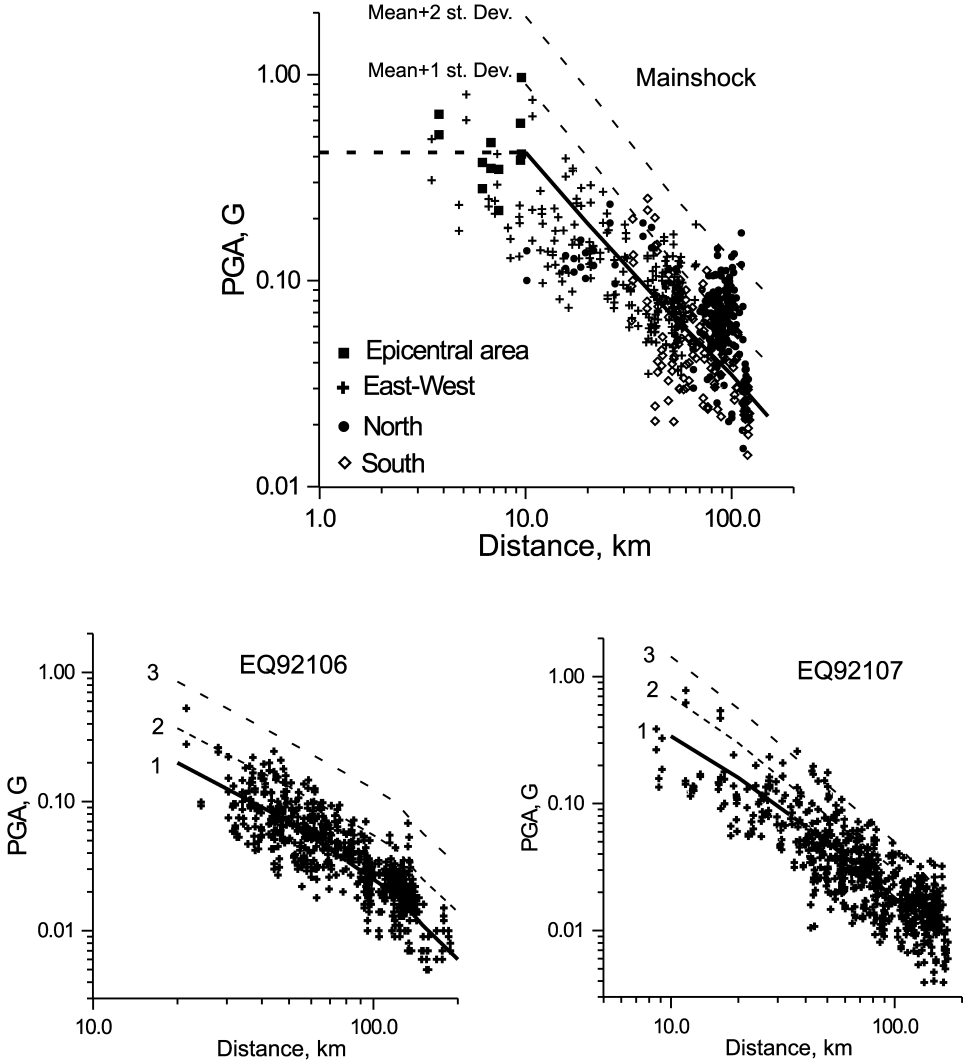


Fig. 5. Comparison between PGA values (horizontal components, symbols) observed during the Chi-Chi earthquake sequence and PGA (lines) predicted using the average soil spectral models and correspondent significant durations (see text). The solid line shows the PGA calculated using the mean values of spectral amplitudes (line 1), and the dashed lines represent the assessments from mean + 1 (line 2) and mean + 2 (line 3) standard deviation spectra. For the mainshock (upper picture) the data from different directions from the source are shown by different symbols.

effective duration. Fig. 5 shows the distribution of the horizontal PGA versus distance for the aftershock with comparison with the modeled values (mean values of the spectral amplitudes, mean + 1 st. dev., and mean + 2 st. dev.). The average value of residuals between the observed data and modeled, using the mean spectra, PGAs (model bias) is about 0.011 and standard deviation of residuals is about 0.19 log unit.

For the case of aftershock EQ92107 the duration $\tau_{0.9}$ also seems to be dependent on distance. The dependence may be described as $\tau_{0.9} = 3.64R^{0.37}$ or $\log_{10}\tau_{0.9} = (0.5 \pm 0.043) + (0.41 \pm 0.023)\log_{10} R$. The comparison between empirical PGA values and those calculated using the average soil spectral model ($6.5 < M_L < 7.0$, $Q(f) = 80f^{0.8}$ )is shown in Fig. 5. The average value of residuals between the observed data and modeled, using the mean spectra, PGAs (model bias) is about $-0.03$, and standard deviation of residuals is about 0.21 log unit.

The comparison between empirical and modeled 5% damped response spectra (averaged empirical spectra and modeled ones) is shown in Fig. 6. The modeled spectra were evaluated from the synthetic acceleration time functions

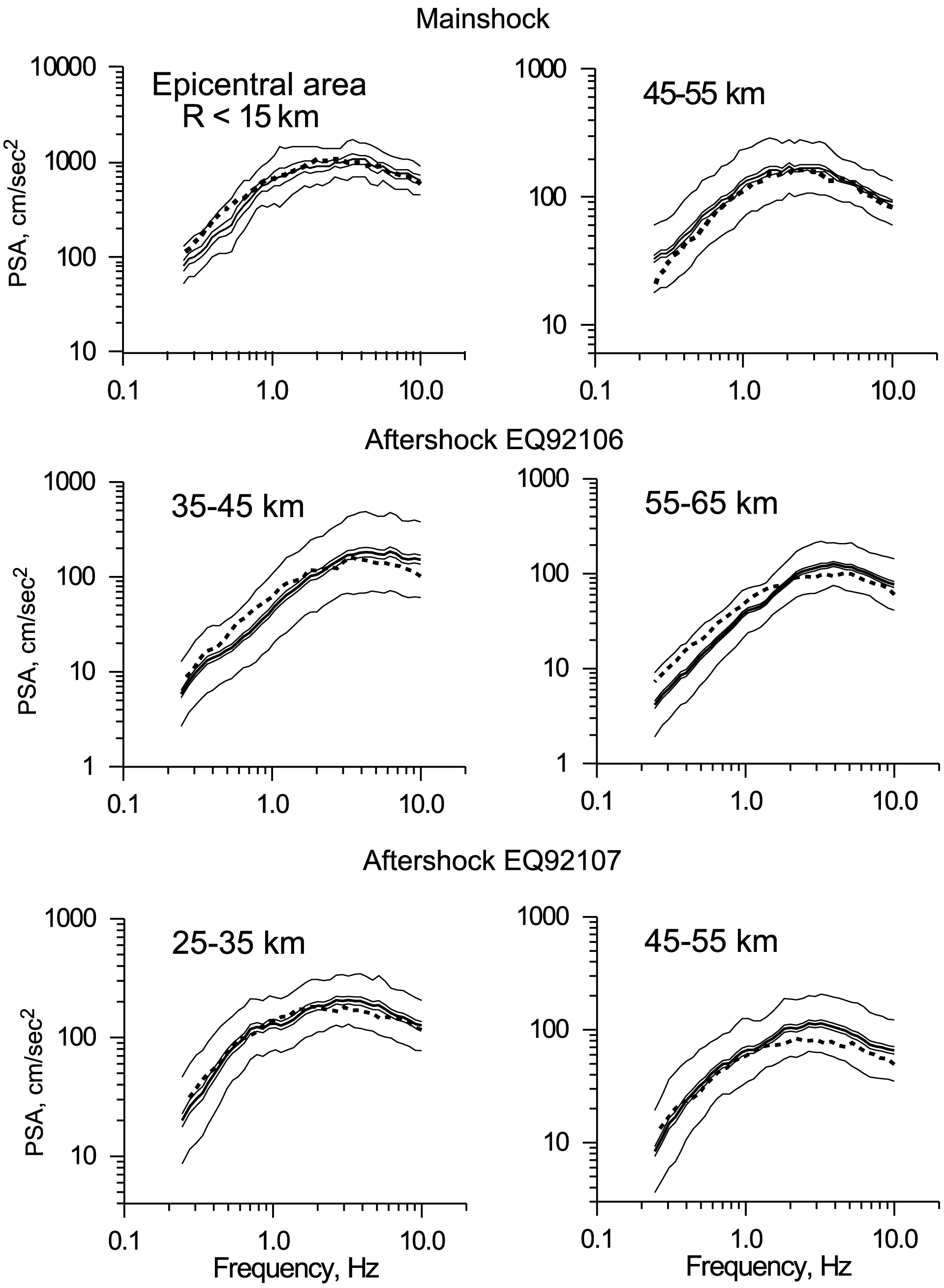


Fig. 6. Comparison between the observed 5% damped response spectra (solid lines, thick line shows mean values, and thin lines—mean ± 1 st. error of means and ± 1 st. deviation limits) and the spectra simulated using average soil spectral model (dashed lines).

(average values). It is seen that the modeled response spectra show a very good agreement with the empirical spectra in the whole considered frequency range.

## 5. Conclusion

The regional empirical model for average soil Fourier amplitude spectra of ground acceleration was developed recently using the Taiwan database from small and moderate earthquakes ($5.0 < M_L < 6.5$). Thus, we attempted to answer the questions: "how well do the available ground motion models predict the observed Chi-Chi motions?". The comparison of the ground motion data collected during the $M_L = 7.3$ Chi-Chi earthquake and large aftershocks allows us to make an affirmative answer to the questions. The application of spectral model, which was evaluated for the correspondent larger interval of local magnitude from the smaller magnitudes data, exhibit a very good agreement with the observations (Fourier amplitude spectra, PGA and response spectra). In the all considered cases, the ground motion parameters predicted using mean + 1 standard deviation spectra provide a reliable upper limit for the observations, and the mean + 2 standard deviation spectra overlap the effect of the Taipei basin response in the case of the mainshock (northern data, distances 90–110 km).

The analyses of the PGA values performed by other authors [21] showed that, when considering the distribution of ground motion parameters versus closest distance to the surface rupture (Chelungpu fault), the overall level of the observed horizontal PGAs from the earthquake are about 50% below the median PGA based on commonly used attenuation in California for $M_W = 7.6–7.7$ [22–24]. The Chi-Chi PGA values are equivalent to what would be predicted for $M_W = 6.6$, 6.0, and 6.2 from Campbell [23], Boore at al. [22] and Sadigh et al. [24] attenuation models, respectively. Unlike the horizontal PGA, the peak ground velocity (PGV) values are relatively high (about 80% higher) than those predicted by existing PGV attenuation model [23]. Therefore, the Chi-Chi earthquake was called as HV-LA (high-PGV, low-PGA) earthquake. However, we have shown that, in general, the average soil spectral model recently developed for the Taiwan region after a certain modification may be applied for prediction of spectral amplitudes and PGA for large earthquakes. The next statement can be directly inferred—the Chi-Chi earthquake and, at least, two large aftershocks (EQ92106 and EQ92107) should be considered as typical, for the Taiwan region, events. The overall level of ground motions at short and intermediate periods (0.1–3.0 s) is not surprisingly weak, quite the contrary, it follows the regional source scaling relations. The only 'surprising phenomenon' of the earthquake is that the short-period ground motions in the region cannot be described by the attenuation models developed for California which are based on moment magnitude values and were derived for strike-slip events. However, it is widely accepted that the attenuation may be different for different seismic regions, and it is necessary to construct region-specific ground motion models.

## Acknowledgments

The study was carried out in National Center for Research on Earthquake Engineering and was supported by the National Science Council of the Republic of China under grant NSC89-2811-E-319-005.

## References

[1] Cheng SN, Yeh YT, Loh CH, Chang CH, Shin TC. Strong-motion data reduction for aftershocks of Chi-Chi earthquake. Proceedings of International Workshop on Annual Commemoration of Chi-Chi Earthquake, September 18–20, NCREE, Taipei, vol. 1; 2000. p. 275–82.
[2] Boore DM, Atkinson GM. Stochastic prediction of ground motion and spectral response parameters at rock sites in eastern North America. Bull Seismol Soc Am 1987;77:440–67.
[3] Atkinson GM, Boore DM. Ground-motion relations for eastern North America. Bull Seismol Soc Am 1995;85:17–30.
[4] Atkinson GM, Silva W. Stochastic modeling of California ground motions. Bull Seismol Soc Am 2000;90:255–74.
[5] Lam N, Wilson J, Hutchinson G. Generation of synthetic earthquake accelerograms using seismological modelling: a review. J Earthquake Engng 2000;4:321–54.
[6] Boore DM. Stochastic simulation of high frequency ground motion based on seismological model of the radiated spectra. Bull Seismol Soc Am 1983;73:1865–94.
[7] Atkinson GM. Earthquake source spectra in eastern North America. Bull Seismol Soc Am 1993;83:1778–98.
[8] Boatwright J, Choy G. Acceleration source spectra anticipated for large earthquakes in northeastern North America. Bull Seismol Soc Am 1992;82:660–80.
[9] Rovelli A, Bonamassa O, Cocco M, Di Bina M, Mazza Z. Scaling laws and spectral parameters of the ground motion in active extensional areas in Italy. Bull Seismol Soc Am 1988;78:530–60.
[10] Tsai CCP. Relationships of seismic source scaling in the Taiwan region. Terrestial, Atmospheric Ocean Sci 1997;8:49–68.
[11] Sokolov V. Spectral parameters of ground motion in different regions: comparison of empirical models. Soil Dynam Earthquake Engng 2000;19:173–81.
[12] Sokolov V, Loh CH, Wen KL. Empirical model for estimating Fourier amplitude spectra of ground acceleration in Taiwan region. Earthquake Engng Struct Dynam 2000;29:339–57.
[13] Chernov YuK. Strong ground motion and quantitative assessment of seismic hazard. Tashkent: Fan Publishing House; 1989. in Russian.
[14] Sokolov V. Ground acceleration spectra from Caucasus earthquakes, Izvestiya. Phys Solid Earth 1998;34:663–75.
[15] Furumura T, Koketsu K, Wen KL, Furumura M. Numerical simulation of strong ground motion during the Chi-Chi, Taiwan, earthquake. Proceedings of International Workshop on Annual Commemoration of Chi-Chi Earthquake, September 18–20, NCREE, Taipei, vol. 1; 2000. p. 222–32.
[16] Huang CT, Chen SS. Near-field characteristics and engineering implications of the 1999 Chi-Chi earthquake. Earthquake Engng Engng Seismol 2000;2:23–41.
[17] Wen KL, Yeh YC. Nonlinear soil response during the 1999 Chi-Chi, Taiwan earthquake. Seismol Res Lett 2001;72:248.

[18] Boore DM. Stochastic simulation of high frequency ground motion based on seismological model of the radiated spectra. Bull Seismol Soc Am 1983;73:1865–94.

[19] Wen KL, Yeh YT. Characteristics of strong motion durations in the SMART1 array area. Terrestial, Atmospheric Ocean Sci 1991;2: 187–201.

[20] Trifunac MD, Brady AG. A study of the duration of strong earthquake ground motion. Bull Seismol Soc Am 1975;65:581–626.

[21] Tsai YB, Huang MW. Strong ground motion characteristics of the Chi-Chi, Taiwan earthquake of September 21, 1999. Earthquake Engng Engng Seismol 2000;2:1–21.

[22] Boore DM, Joyner WB, Fumal TE. Equations for estimating horizontal response spectra and peak acceleration from western north American earthquakes: a summary of recent work. Seismol Res Lett 1997;68:128–53.

[23] Campbell KW. Empirical near-source attenuation relationships for horizontal and vertical components of peak ground acceleration, peak ground velocity, and pseudo-absolute acceleration response spectra. Seismol Res Lett 1997;68:154–79.

[24] Sadigh K, Chang CY, Egan JA, Makdisi F, Youngs RR. Attenuation relationships for shallow crustal earthquakes based on California strong-motion data. Seismol Res Lett 1997;68:180–9.